LUNDS UNIVERSITET
Lunds Tekniska Högskola

INVESTIGATION OF HEAT TRANSFER AND MASS TRANSFER PARAMETERS IN A CONVECTION OVEN FOR MODEL FOODS

Submitted by
Chandana Mysore Somashekar
(ch7445my-s@student.lu.se)

Department of Food Technology, Engineering and Nutrition
Faculty of Engineering, LTH
Lund University

Supervisor: *Andreas Håkansson*
Examiner: *Marilyn Rayner*

August 2020

LUND-SWEDEN

Abstract

Forced air convection systems are the most preferred design of choice in many of the industrial-scale convection ovens. In this study, experimental investigation on convective heat transfer and mass transfer within a forced air convection oven was performed at different oven temperatures (100℃, 110℃ and 120℃) and at flow velocity (2m/s, 3m/s and 4m/s) using potato slices (10*10*60mm) as model food. The Yıldız et al., 2007 approach with slight modification was applied to estimate the effective convective heat transfer and mass transfer coefficient during convection frying. In addition to the experimental approach, the empirical correlation method was also used to calculate the convective heat transfer and mass transfer coefficient and compared with the coefficient values obtained from the experimental method. The effective heat transfer and mass transfer coefficient obtained from the Yıldız et al., 2007 method was found to be almost constant with increasing oven temperature. However, with increasing flow velocity the effective heat transfer coefficient increased but the influence of flow velocity on effective mass transfer coefficient was not significant. The comparison of the coefficient values obtained from the experimental method and the empirical correlations showed that the experimental method yields quite low values than the empirical method.

Acknowledgements

It gives me immense pleasure to present this section as a tribute to all the people who encouraged and supported me during this degree project.

This study was carried out as a degree project in food engineering at the Department of Food Technology, Engineering and Nutrition under the supervision of Associate Professor Andreas Håkansson. The examiner of the project is Professor Marilyn Rayner, Department of Food Technology, Engineering and Nutrition.

Firstly, I would like to express my sincere gratitude to my supervisor Prof. Andreas Håkansson for giving me the opportunity to carry out this project and guiding me by providing his valuable suggestions and feedback throughout the project. Secondly, I would like to thank Grant Thamkaew Doctoral student at Department of Food Technology, Engineering and Nutrition for providing instructions required to operate the convection oven and cooperating during the entire project.

Finally, I thank Almighty for being able to give my best and my special thanks go to my parents and friends for their constant moral support and encouragement which helped me to successfully completion this project.

Index

Nomenclature

A	Surface area (m^2)
B_i	Biot number
$C_{(x,t)}$	Moisture content at any point and any time (kg/kg solid)
C^*_{∞}	Moisture content in the air (kg/m^3)
C^*_{sur}	Moisture content at the surface (kg/m^3)
C_{∞}	Moisture content of the air in the oven (kg/kg solid)
C_i	Initial uniform moisture content of the product (℃)
C_p	Specific heat (J/kgK)
D	Moisture diffusivity (m^2/s)
d_c	Characteristic dimension
h	Heat transfer coefficient (W/m^2K)
h_{eff}	Effective heat transfer coefficient (W/m^2K)
k	Thermal conductivity
k_m	Mass transfer coefficient (m/s)
L	Half thickness (m)
m_B	Mass flux (kg/s)
N_{Nu}	Nusselt number
N_{Pr}	Prandtl number
N_{Re}	Reynolds number
N_{Sc}	Schmidt number
N_{Sh}	Sherwood number
Q	Heat flux (W)
St	Stanton number
t	Time (s)
$T_{(x,t)}$	Temperature at any point and any time (℃)
T_{∞}	Temperature of the air in the oven (℃)
T_{air}	Temperature of the air (℃)
T_f	Film temperature (℃)
T_i	Initial uniform temperature of the product (℃)
T_{sur}	Temperature at the product surface (℃)
u	Velocity (m/s)
V	Volume (m^3)
x	Location where temperature is measured in infinite slab ($0 \leq x \leq L$)
y	Location where temperature is measured in infinite slab ($0 \leq y \leq L$)
α	Thermal diffusivity (m^2/s)
ρ	Density (kg/m^3)
ΔH_{evp}	Enthalpy of vaporization (kJ/mol)
$\frac{dm}{dt}$	Rate of mass reduction (kg/s)
μ	Viscosity (Ns/m^2)
μ_b	Viscosity of the fluid(air) (Ns/m^2)
μ_w	Viscosity at the solid surface (Ns/m^2)

1. Introduction

1.2 Background

A forced convection oven is popular cooking equipment used in the home and in the food industries to produce baked products, meat, dried and fried products. There are various types of forced convection ovens available in the market. In these ovens, food is heated by hot air that is circulated around the product by a fan fit to the oven wall. Heat is transferred to the product through radiation and convective heat transfer by the circulating air, at same time water from the product surface is transferred to the air due to evaporation (Skjoldebrand, 1980). In many solid foods processes heat transfer is analogous to mass transfer and there is a strong coupling between heat and moisture transfer. Such a process is called as a coupled heat and mass transfer. This coupled heat and mass transfer play an important role in many solid food processes like baking, drying, and frying (Feyissa, 2011).

During frying in a convection oven, the product is heated by air at high temperature to induce changes in the product like water evaporation, crust formation, browning, protein denaturation and inactivation of enzymes and various microorganisms. These changes are desirable and renders the product with appealing colour, flavour, texture, and shelf life. However, some undesirable transformation may also occur for example, the formation of acrylamide, which is regarded as a potentially carcinogen. The acrylamide formation depends upon temperature and heating time (Feyissa, 2011). Mass transfer in convection oven refers to the loss of water content from solid food which has a major influence on the chemical and physical properties that describes the desired food quality and safety (Thorvaldsson and Skjöldebrand, 1996). Therefore, it is essential to have a thorough quantitative understanding of mass transfer and heat transfer parameters during cooking food. Further, understanding of process parameters helps to identify and apply optimal processing conditions to obtain desired final product quality and has an important role in scale up at industry.

Several studies on heat and mass transfer coefficients and the effects of influencing factors are present in the literature. (Skjoldebrand, 1980; Yıldız et al., 2007; Safari et al., 2018). These studies have contributed a lot of useful information about heat and mass transfer using different techniques. However, the study of heat transfer and mass transfer parameters in a forced convection oven is limited.

1.3 Objectives

- Investigation of effective heat transfer and mass transfer coefficient at different temperatures and flow(air) velocity using the Yildiz et al. (2007) approach in a forced air convection oven for cuboidal model foods.
- Discuss and conclude on how the effective heat transfer and mass transfer coefficients vary with increasing oven temperature and flow(air) velocity.

- Compare the experimentally obtained coefficient values (using method described in Yıldız et al., 2007) with the values from the empirical correlations and discuss the variations.

2. Theory

2.1 Heat transfer

Heat transfer is the movement of energy from one point to another by the virtue of difference in temperature. This temperature difference is the driving force which establishes the rate of heat transfer (Toledo, 2007). Heat transfer is of two types, external heat transfer and internal heat transfer. The former takes place between the heating medium and the solid food and the latter takes place within the solid food itself. A solid food and a heating medium exchanges heat at their boundaries by the mechanism of conduction, convection, or radiation (Feyissa, 2011). When the heat is transferred by the molecule that move from one point to another and exchanges energy with another molecule in other location, the process is called convection heat transfer (Toledo, 2007). There are two types of convective heat transfer depending on the flow characteristics of the heating medium: forced convection and free convection. In forced convection, the flow is artificially induced by blowing air or pumping liquid on the heating or cooling surface. In contrast, free convection occurs due to density and viscosity changes associated with the temperature difference in the fluid (Heldman and Lund, 2007). Convective heat transfer is a major mode of heat transfer between the surface of a solid food and the surrounding heating medium, used in many processes like baking, roasting and frying in a convection oven (Heldman and Lund, 2007; Feyissa, 2011). In domestic convection ovens, radiation mode of heat transfer is considered to have major contribution. In case of convection heat transfer, the rate of heat transfer is proportional to the surface area in contact with the heating medium and the temperature difference and is expressed as,

$$Q = h*A*(T_{air}-T_{sur}) \qquad \text{Eq. (1)}$$

where 'h' is the heat transfer coefficient($W \cdot m^{-2} \cdot K^{-1}$), 'A' is the area of the heating medium – solid interface where heat is being transferred (m^2), T_{air} is the temperature of the air in the oven (K), $T_{sur}$is the surface temperature of the solid food (K). Convective heat transfer during forced air convection is represented as heat transfer through a thin film of air that possess a temperature gradient, at the air-solid surface interface. The thin air film is a boundary layer that resists the heat flow between the air stream and the solid food. The reduction in the thickness of the boundary layer will promote the heat transfer to the solid food. The heat transfer coefficient depends on the thermophysical properties of the fluid, the velocity of the fluid flow, geometry of the solid undergoing heating or cooling and the roughness of the surface in contact with the fluid flow. The convective heat transfer coefficient, h, has been measured experimentally by several researchers using different methods for a variety of operating conditions. Empirical correlations have been developed to estimate the convective heat transfer coefficient for different operating conditions (Singh and Heldman, 2014).

2.2 Mass transfer

Mass transfer in food systems is referred as, the migration of a constituent of a fluid or a component of a mixture. The migration occurs because of changes in the physical equilibrium of the system caused by the concentration differences. It can occur within one phase or may involve transfer from one phase to another. Mass transfer involves both diffusion at a molecular level and bulk transport of mass due to convection flow (Singh and Heldman, 2014). Diffusion is the process by which matter is transported from one part of the system to another due to random molecular motion (Toledo, 2007). The diffusion process is described mathematically using Fick's law of diffusion, which states that the mass flux per unit area of a component is proportional to its concentration gradient. Convection enhances the transport of components due to concentration gradient as a result, the mass flux of the component will be higher than would occur by molecular diffusion (Singh and Heldman, 2014). During forced convection, air flows over a wet surface and water is transferred from the surface to the air which is analogous to convection heat transfer. Therefore, the driving force for mass transfer is a concentration difference, and the proportionality constant between the mass flux and the driving force is the mass transfer coefficient.

$$\frac{\dot{m}_B}{A} = k_m \, (C^*_{sur} - C^*_{\infty}) \qquad \text{Eq. (2)}$$

'k_m' is convective mass transfer coefficient defined as, the rate of mass transfer per unit area per unit concentration difference. 'm_B' is the mass flux (kg/s), 'C*' is moisture content in (kg water/m^3), 'A' is area of the surface through which water is transferred to air (m^2). The determination of mass transfer coefficient is analogous to that of heat transfer coefficient, involving the dimensionless analysis. (Singh and Heldman, 2014).

2.3 Simultaneous heat and mass transfer

Convection cooking involves the simultaneous heat and mass transfer. Heat is transferred mainly by convection from air to the product surface, and by conduction from the surface toward the product centre. Meanwhile, moisture diffuses outward toward the product surface, and is vaporized. At the product surface, simultaneous heat and mass transfer is controlled by convective processes(Singh and Heldman, 2014). Heat transferred from the air to the product surface results in evaporation of water from the surface. This evaporation process requires heat energy, which is taken away by the molecules when they convert from liquid phase to the gas phase and escape from the surface. Since the molecules take away heat while leaving the surface, this has a cooling effect on the surface which is referred to as evaporation cooling effect. This phenomenon is mainly because of coupling between heat transfer (air to product) and mass transfer(product to air) (Toledo, 2007). There is also a coupling in the other direction since the heat transfer influences the fluid (air) temperature which influences the thermophysical properties of the fluid(air). This type of coupling effect is mostly observed in food processes involving air flow. For example, freezing, thawing, dehydrating, and cooking of food products (Kondjoyan & Daudin, 1997). These coupling

effects introduce the concept of effective heat transfer coefficient. Effective heat transfer coefficient is a combination of convective heat transfer coefficient and evaporative cooling. While determining effective heat transfer coefficient, heat exchanged by radiation or by phase change when it occurs(evaporation cooling effect) is considered in addition to the heat exchanged by convection (Kondjoyan & Daudin, 1997). The effective heat transfer coefficient provides the heat interaction between the product and the heat transfer fluid during heat or cooling processes (Chen et al., 1999). It can be represented as,

$$h_{eff} * A * (T_{air} - T_{sur}) = h * A * (T_{air} - T_{sur}) + \Delta H_{vap} * \frac{dm}{dt} + radiation \qquad \text{Eq.(3)}$$

2.4 Methods to determine the convective heat transfer and mass transfer parameters

Over the year's researchers have used different methods to determine the heat transfer and mass transfer parameters in a various operating condition. There is no standard method for measuring heat and mass transfer coefficients during forced convection cooking (J.K. Carson et al., 2006; Sablani, 2009). In this study, we have used the technique discussed in Yıldız et al. (2007) for immersion frying to calculate the heat and mass transfer coefficients during forced convection cooking. In Yıldız et al. (2007) method the experimental data were used to determine the heat and mass transfer parameters during frying from the dimensionless temperature and concentration ratio plots, respectively. Another approach used in this study is, calculating heat transfer and mass transfer coefficient using empirical equations or correlations. This approach is applicable when appropriate correlations suitable for the type of process and food of interest are available.

2.4.1 Yıldız et al. (2007) method for determination of heat transfer coefficient

In this method, the temperature in the centre of the sample is measured as a function of time and used together with an analytical solution to back-calculate the rate of external heat transfer. Eq. (4) is the partial differential equation for heat conduction.

$$\frac{\partial^2 T}{\partial x^2} = \frac{1}{\alpha}\frac{\partial T}{\partial t} \quad , \quad 0 \le x \le L \quad \text{for } t > 0 \qquad \text{Eq. (4)}$$

Eq. (4) is solved by applying boundary conditions given in Eq. (5)

Eq. (5)

$$\left.\frac{\partial T}{\partial x}\right|_{x=0} = 0 \qquad -k\left.\frac{\partial T}{\partial x}\right|_{x=L} = h(T|_{x=L} - T_\infty) \qquad T|_{t=0} = T_i$$

Eq. (6) is the analytical solution of Eq. (4).

$$\left(\frac{T_{(x,t)} - T_\infty}{T_i - T_\infty}\right) = \sum_{n=1}^{\infty} \frac{2 \sin \mu_n}{\mu_n + \sin \mu_n \cos \mu_n} \cdot \cos\left(\mu_n \frac{x}{L}\right) \exp\left(-\mu_n^2 \frac{\alpha t}{L^2}\right) \qquad \text{Eq. (6)}$$

$$B_i = \mu_n \tan \mu_n \qquad \text{Eq. (6b)}$$

Eq. (6) gives temperature as a function of time at any point in an infinite slab.
After a certain interval of processing time where the Fourier number ($\alpha t/L^2$) is greater than 0.1, Eq. (6) converges to the first term in the series. The first term solution for a cuboidal shaped solid is obtained by the product of the first term solutions of three infinite slabs of the same thickness. Eq. (7) represents the solution for a cuboidal shaped food.

$$\left(\frac{T_{(x,t)}-T_\infty}{T_i-T_\infty}\right)\cdot\left(\frac{T_{(y,t)}-T_\infty}{Ti-T_\infty}\right)=\mathrm{A}\exp\left(-2\mu_1^2\frac{\alpha t}{L^2}\right) \quad \text{Eq. (7)}$$

Where A = $\left(\frac{2\sin\mu_1}{\mu_1+\sin\mu_1\cos\mu_1}\right)^2\cdot\cos\left(\mu_1\frac{x}{L}\right)\cdot\cos\left(\mu_1\frac{y}{L}\right)$

Taking natural logarithm on both sides of Eq. (7) gives Eq. (8)

$$ln\left(\frac{T_{(x,y,t)}-T_\infty}{T_i-T_\infty}\right)=\ln\mathrm{A}-2\mu_1^2\frac{\alpha t}{L^2} \quad \text{Eq. (8)}$$

The slope of linear section of $ln\left(\frac{T_{(x,y,t)}-T_\infty}{T_i-T_\infty}\right)$ versus time is used in solving Eq. (8) for μ_1 value. The thermal diffusivity α is calculated from the thermophysical properties of food sample(potato) presented in table 1.1 in Appendix A. Further the heat transfer coefficient, h, and heat transfer Biot number (Bi_h) are determined by using Eq. (9) and Eq. (10) where k is the thermal conductivity of potato in (W/mK).

$$B_{ih}=\mu_1\tan\mu_1 \quad \text{Eq. (9)}$$

$$B_{ih}=\frac{hL}{k} \quad \text{Eq. (10)}$$

2.4.2 Yıldız et al. (2007) method for determination of mass transfer coefficient

The mass transfer coefficient is determined from the dimensionless concentration versus time plots. This approach relies on measuring moisture content of the sample over time and solving differential equation (Eq. (11)) using boundary conditions in Eq. (12)

$$\frac{\partial^2 C}{\partial x^2}=\frac{1}{D}\frac{\partial C}{\partial t}\ ,\quad 0\le x\le L\quad \text{for } t>0 \quad \text{Eq. (11)}$$

$$\left.\frac{\partial C}{\partial x}\right|_{x=0}=0\qquad -D\left.\frac{\partial C}{\partial x}\right|_{x=L}=k_C(C|_{x=L}-C_\infty)\qquad C|_{t=0}=C_i \quad \text{Eq. (12)}$$

Eq. (13) is the solution of differential equation(Eq. (11)) that gives concentration as a function of time and location for an infinite plate.

$$\left(\frac{C_{(x,t)}-C_\infty}{C_i-C_\infty}\right)=\frac{2\sin^2\mu_1}{\mu_1[u_1+\sin\mu_{1^*}\cos\mu_1]}\cdot\cos\left(\mu_n\frac{x}{L}\right)\exp\left(-\mu_n^2\frac{Dt}{L^2}\right) \quad \text{Eq. (13)}$$

For a long processing time, $F_o = \alpha t/L^2$ is greater than 0.1 and the first term of the differential equation solution(Eq. (13)) is enough to give accurate results. Note that the time interval for

which the value of Fourier number($\alpha t/L^2$) is greater than 0.1 is different for mass and heat transfer.

By integrating Eq.(13) throughout the whole volume $\left(\frac{1}{V}\int_0^V C(x,t)\,dV\right)$, the equation for average moisture concentration in a cuboid shaped solid(Eq. (14)) was obtained.

$$\left(\frac{\bar{C}(t)-C_\infty}{C_\iota-C_\infty}\right)=\frac{2\sin^2\mu_1}{\mu_1[u_1+\sin\mu_{1^*}\cos\mu_1]}\exp\left(-\mu_1^2\frac{Dt}{L^2}\right) \quad \text{Eq. (14)}$$

$\bar{C}(t)$ is the average moisture content at time t in (kg/kg solids)
Taking the natural logarithm on both the sides of Eq. (14) gives the following equation:

$$ln\left(\frac{\bar{C}(t)-C_\infty}{C_\iota-C_\infty}\right)=2\,ln\,E-2\mu_1^2\frac{Dt}{L^2} \quad \text{Eq. (15)}$$

Where, E = $\frac{2\sin^2\mu_1}{\mu_1[u_1+\sin\mu_{1^*}\cos\mu_1]}$

According to Yıldız et al. (2007) method, a plot of $ln\left(\frac{\bar{C}(t)-C_\infty}{C_\iota-C_\infty}\right)$ against time is used to determine the moisture diffusivity, D (m^2/s) and μ_1 from the slope and the intercept of the plotted curve, respectively . However, preliminary investigations showed that the method was extremely sensitive to small deviations in the measured data. Hence, in this study a bit modified method similar to the one in Yıldız et al. (2007) for heat transfer is used. By applying similar approach as in heat transfer, a plot of $ln\left(\frac{\bar{C}(t)-C_\infty}{C_\iota-C_\infty}\right)$ against time is used to determine μ_1 value, from the slope of the plotted curve. The moisture diffusivity, D (m^2/s) is assumed to be constant and the value is obtained from Yıldız et al. (2007) . After determining μ_1, the mass transfer Biot number (Bi_m) and mass transfer coefficient (k_m) were obtained from Eq. (16).

$$Bi_m=\mu_1\,tan\,\mu_1=\frac{k_mL}{D} \quad \text{Eq. (16)}$$

2.4.3 Determination of heat transfer coefficient using dimensionless correlations

Convective heat transfer coefficient, 'h', can be estimated from dimensionless correlations based on the velocity and thermophysical properties of the air and the geometrical shape and temperature of the food. The general correlation between the dimension less numbers for forced convection is,

$$N_{Nu} = f(N_{Re}, N_{Pr}) \quad \text{Eq. (17)}$$

Where, N_{Nu} is Nusselt number ,N_{Pr} is the Prandtl number and N_{Re} is Reynold number.
The Nusselt number,

$$N_{Nu} = \frac{h\,d_c}{k} \quad \text{Eq. (18)}$$

Where h is convective heat-transfer coefficient(W/[m^2K]), d_c is the characteristic dimension (m), k is thermal conductivity of fluid (W/[mK]) is defined as the ratio of the characteristic dimension of a system and the thickness of the boundary layer of fluid that would transmit heat by conduction at the same rate as that calculated using the heat transfer coefficient. The Reynolds number,

$$N_{Re} = \frac{\rho u\, d_c}{\mu} \qquad \text{Eq. (19)}$$

where ρ is density of fluid (kg/m^3), u is velocity of fluid (m/s), μ is viscosity (Pa s) is described as the ratio of inertial forces to the frictional forces. Prandtl number is the ratio of rate of momentum exchange between molecules and the rate of energy exchange between molecules that lead to the transfer of heat,

$$N_{Pr} = \frac{\mu\, C_p}{k} \qquad \text{Eq. (20)}$$

Where C_p is specific heat (J/ [kg K]) and k is thermal conductivity of fluid (W/[mK]).
With a basic understanding of these three dimensionless numbers, correlations for determining 'h', convective heat-transfer coefficient(W/[m^2K]) during various operating conditions are obtained. Different correlations are obtained, depending on whether the flow is laminar or turbulent. Some of the correlations that are relevant to the operating conditions of this study are, flow over cylinder of noncircular cross section, flow around a cylinder and flow around a sphere. (Singh and Heldman, 2014; Toledo, 2007; Bergman and Lavine, 2018)

Eq.(21) is the Nusselt correlation for predicting heat transfer coefficient value for flow over cylinders of noncircular cross section with characteristic length d_c (m) ('d_c' is half thickness for cuboid geometry) and all thermophysical properties of fluid(air) evaluated at film temperature, T_f =[(T_s+T_{air})/2]. Figure 1 is a schematic illustration of the fluid flow around a cylinder of noncircular cross section(cuboid) giving rise to the external convective heat transfer described by Eq. (21). The constant values are taken from table 1.2 appendix A (Bergman and Lavine, 2018).

$$N_{Nu} = C(N_{Re})^m(N_{Pr})^{1/3} \qquad \text{Eq. (21)}$$

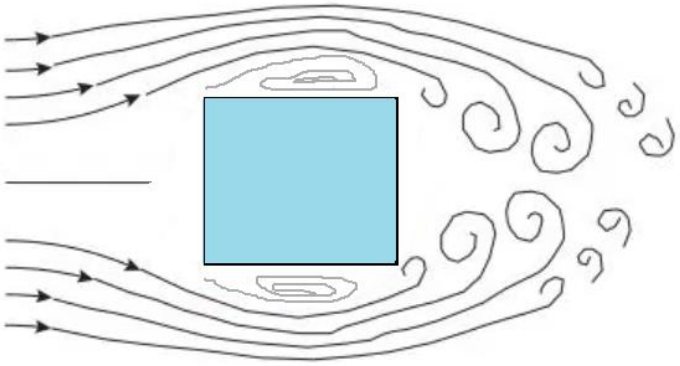

Figure 1. Illustration of flow over cylinders of noncircular cross section

The Nusselt correlation for determining the convective heat transfer coefficient for flow around a sphere, when the single sphere is heated or cooled is,

$$N_{Nu} = 2 + 0.6(N_{Re})^{0.5}(N_{Pr})^{0.33} \qquad \text{Eq. (22)}$$

for $1 < N_{Re} < 70000$ and $0.6 < N_{Pr} < 400$

where the characteristic dimension, d_c, is the outside diameter of the sphere. The fluid properties are evaluated at the film temperature T_f (Singh and Heldman, 2014). Figure 2 shows an illustration of the fluid flow around spherical and cylindrical object which results in the external convective heat transfer described by Eq. (22) and Eq. (23) respectively.

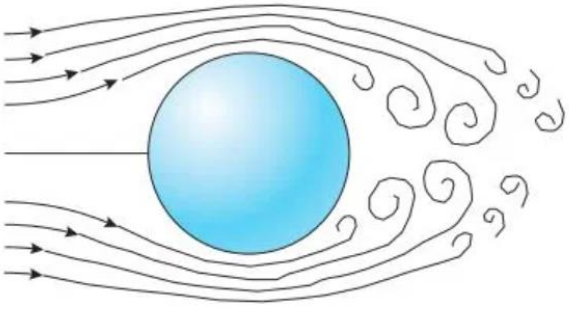

Figure 2.Illustration of flow around sphere and cylinder

Eq. (23) is the Nusselt number correlation for flow around a cylinder.

$$N_{Nu} = (0.4N_{Re}^{1/2} + 0.06N_{Re}^{2/3})(N_{Pr})^{0.4}\left(\frac{\mu_b}{\mu_w}\right)^{1/4} \qquad \text{Eq. (23)}$$

In the range $1.0 < Re < 1.0*10^5$, $0.67 < Pr < 300$ and $0.25 < \frac{\mu_b}{\mu_w} < 5.2$

All fluid properties are evaluated at the film temperature T_f ,except μ_w , which is evaluated at wall temperature and the characteristic dimension, d_c, is the outer diameter of the cylinder.(Bird, 2002)

In this study Eq. (21), Eq. (22) and Eq. (23) are used to determine to heat transfer coefficient, h, during forced convection cooking of a cuboidal shaped potato slices and the value obtained are compared to with the experimentally determined results.

2.4.4 Analogy between heat and mass transfer - Chilton and Colburn analogy

The Chilton-Colburn analogy states that there is a relationship between the rate of convective heat and mass transfer, provided a number of assumptions are met (e.g., that all physical properties of the food and the air remains constant with respect to time).

$$\mathrm{St} \cdot \mathrm{Pr}^{2/3} = \mathrm{St_m} \cdot \mathrm{Sc}^{2/3} \qquad \text{Eq. (24)}$$

where St and St_m are the heat transfer Stanton number and mass transfer Stanton number, respectively.

$$\mathrm{St} = \frac{\mathrm{Nu}}{\mathrm{Re} \cdot \mathrm{Pr}} \qquad \text{Eq. (25)}$$

$$\mathrm{St_m} = \frac{\mathrm{Sh}}{\mathrm{Re} \cdot \mathrm{Sc}} \qquad \text{Eq. (26)}$$

By substituting the equations 25 & 26 in Eq. (24)

$$\frac{\mathrm{Nu}}{\mathrm{Re} \cdot \mathrm{Pr}} \cdot \mathrm{Pr}^{2/3} = \frac{\mathrm{Sh}}{\mathrm{Re} \cdot \mathrm{Sc}} \cdot \mathrm{Sc}^{2/3} \qquad \text{Eq. (27)}$$

$$\mathrm{Nu} \cdot \mathrm{Pr}^{-1/3} = \mathrm{Sh} \cdot \mathrm{Sc}^{-1/3} \qquad \text{Eq. (28)}$$

$$\mathrm{Sh} = \mathrm{Nu} \cdot \mathrm{Pr}^{-1/3} \cdot \mathrm{Sc}^{1/3} \qquad \text{Eq. (29)}$$

By substituting the Nusselt number from the heat transfer correlation in Eq. (29) we get the Sherwood number. The mass transfer coefficient is calculated from the Sherwood number.

2.4.5 Determination of mass transfer coefficient using dimensionless correlations

Convective mass transfer coefficient 'k_m' is determined using dimensionless correlations, analogous to the correlations used in convective heat transfer coefficient estimation. some of the important dimensionless numbers involved in determination of mass transfer coefficient are, Sherwood number (N_{Sh}), Schmidt number (N_{Sc}) and Reynold number (N_{Re}). The functional relationship that correlate these dimensional numbers for forced convection is,

$$N_{Sh} = f(N_{Re}, N_{Sc}) \qquad \text{Eq. (30)}$$

$$N_{Sh} = \frac{k_m \cdot d_C}{D_{AB}} \qquad \text{Eq. (31)}$$

k_m is the mass transfer coefficient (m/s), dc is the characteristic dimension (m), D_{AB} is diffusivity for component A in fluid B.

$$N_{Re} = \frac{\rho \cdot u \cdot d_c}{\mu} \quad \text{Eq. (32)}$$

ρ is density of fluid (kg/m^3), u is velocity of fluid (m/s), μ is viscosity (Pa s).

$$N_{Sc} = \frac{\mu}{\rho D_{AB}} \quad \text{Eq. (33)}$$

As the heat transfer is analogous to mass transfer, the Chilton-Colburn analogy described in section 2.4.4 is used to obtain the mass transfer coefficient value from the heat transfer correlations.

By Applying the Chilton and Colburn analogy, Eq. (34) gives the convective mass transfer coefficient, (k_m) for flow over cylinders of noncircular cross section

$$N_{Sh} = C(N_{Re})^m \cdot N_{Sc}^{1/3} \quad \text{Eq. (34)}$$

All fluid properties are evaluated at the film temperature T_f and d_c for a cuboid shaped solid is half the thickness. The values of C and m, are obtained from table 1.1 appendix A.

The dimensionless correlation for estimating the mass transfer coefficient in case of flow over spherical objects is,

$$N_{Sh} = 2 + 0.6(N_{Re})^{0.5} \cdot N_{Sc}^{1/3} \quad \text{Eq. (35)}$$

where the characteristic dimension, d_c, is the outer diameter of the sphere. The fluid properties are evaluated at the film temperature T_f.

The dimensionless correlation for estimating the mass transfer coefficient for flow around a cylinder is given by Eq. (36),

$$N_{Sh} = (0.4N_{Re}^{1/2} + 0.06N_{Re}^{2/3})(N_{Pr})^{0.4}\left(\frac{\mu_b}{\mu_w}\right)^{1/4} \cdot N_{Pr}^{-1/3} \cdot N_{Sc}^{1/3} \quad \text{Eq. (36)}$$

The characteristic dimension, d_c, is the outer diameter of the cylinder and the fluid properties are evaluated at the film temperature T_f ,except μ_w, which is evaluated at wall temperature.

3. Materials and Methods

3.1 Apparatus

A convection oven specially designed for research purpose (Skjoldebrand,1980) is used in this study (Figure 3). The oven is of dimension 325*325*325 mm and is provided with a mesh plate where the sample is placed. A weighing balance (Samo Tronic Vågsystem AB, Malmo) with uncertainty ±0.5 grams is fixed in the cavity below the oven and the mesh plate inside the oven is connected to the balance. The loss of moisture from the sample during cooking is measured by the balance. The air temperature in the oven is measured by a chromel-alumel thermocouple and can be regulated between 20-400°C.

Figure 3. Convection oven used in the study

3.2 Sample preparation

The experimental trails are performed using the large size potatoes purchased from the local supermarket. The potatoes where peeled and cut into slices(10mm*10mm) using a pommes frites cutter. Slices with proper shape and size where chosen and were cut to a length of 60mm. Eight slices of potato with dimension 10mm*10mm*60mm were used in all the experimental trails.

3.3 Experimental setup

The experimental setup is made using a stainless-steel grill rack to place the potato slices in a suspended manner inside the oven during the entire experimental time. A thread is sewn into the potato slice using a long needle. The thread is then fastened at the bottom end of the potato slice using a toothpick (as shown in figure 4) and both the ends of the thread is tied to the grill rack. The length of the thread is adjusted to make sure the potato slices are at the centre of the grill rack. Every experimental trail is done with eight slices of potato weighing between 50-60g approximately. The slices tied to the grill rack in a suspended manner as illustrated in figure 5. The change in the mass of the sample during the entire experimental

time is recorded by connecting the digital balance to the computer, logging one value per second.

In the experiments involving recording of temperature change in the sample, type-k thermocouples were used. The thermocouple is sewn into two potato slices out of eight using a long needle and sewing thread, making sure that the thermocouple is at the centre of the potato slice. The thread is then fastened using a toothpick and tied to the grill rack. The pictures of the experimental setup with the thermocouple inserted inside the potato slices can be found in appendix F. The centre temperature of the sample during the experiment was recorded by connecting the thermocouple data logger (Pico technology, Eaton Socon, UK) to a computer with the logging software, logging one value per second.

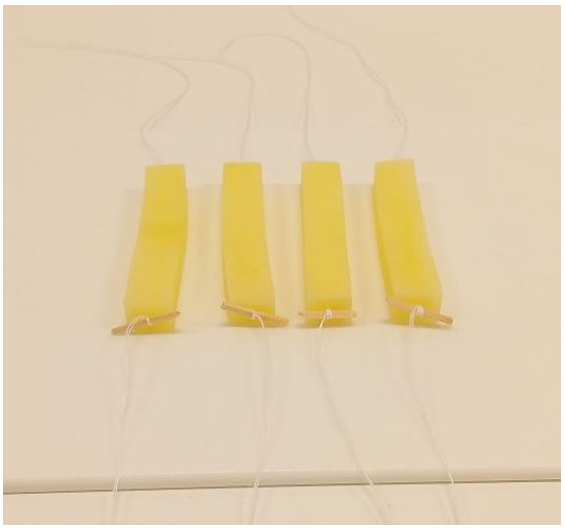

Figure 4.slices of potato with a thread sewn into each piece and fastened at the bottom using a toothpick.

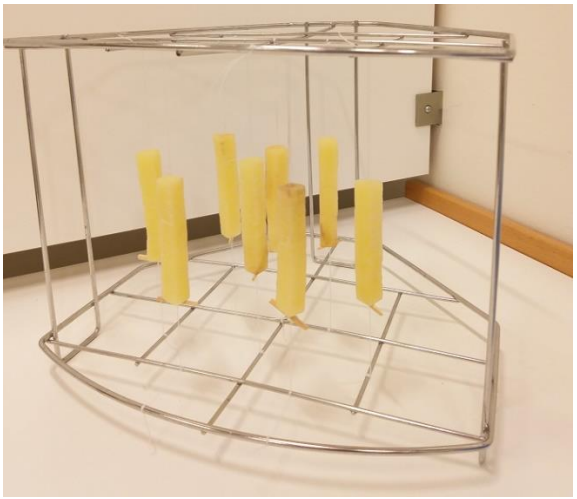

Figure 5. The pieces of potato tied at the centre of the stainless-steel grill rack with the help of the thread that is sewn into each piece.

3.4 Experimental procedure

The weight of empty stainless-steel grill rack is recorded and then weighted again along with the potato slices just before placing it inside the oven. The initial mass of the sample is calculated by subtracting the mass of the empty grill rack from the mass of grill rack with the sample. The oven temperature and air velocity were set and allowed to stabilize for 45min before placing the sample in the oven. Once the sample was place inside the oven the temperature logging and mass logging were started. The schematic representation of the experimental setup is shown in figure6. The runtime for each trial was set to 7200s so that adequate amount of data is recorded. The experimental raw data is retrieved, and calculations are done following the method in section 2.4.1 and section 2.4.2 to estimate the heat transfer coefficient and mass transfer coefficient values using Microsoft Excel.

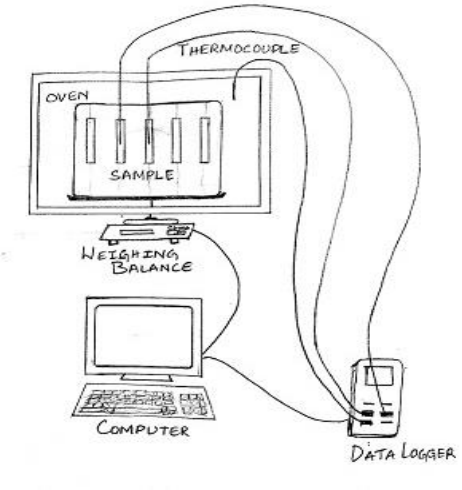

Figure 6. Schematic representation of the experimental setup

The experiments are performed with minimum 3 replicates for each set of condition as represented in table 1. The experimental data of both heat and mass transfer can be recorded simultaneously.

Table 1. Experimental trails performed

Convection cooking with operating conditions (temperature and air velocity)	Replicates
100℃, 3m/s	4
110℃, 3m/s	4
120℃, 3m/s	3
2m/s, 110℃	4
3m/s, 110℃	3
4m/s, 110℃	3

4. Results and Discussion

4.1 Primary results of mass loss and centre temperature increase

The experimental data for the product centre temperature and mass change was recorded simultaneously throughout the run time. Figure 7 is an example of experimental results showing the centre temperature and mass change profile for an oven temperature set 120℃ and air velocity 3m/s.

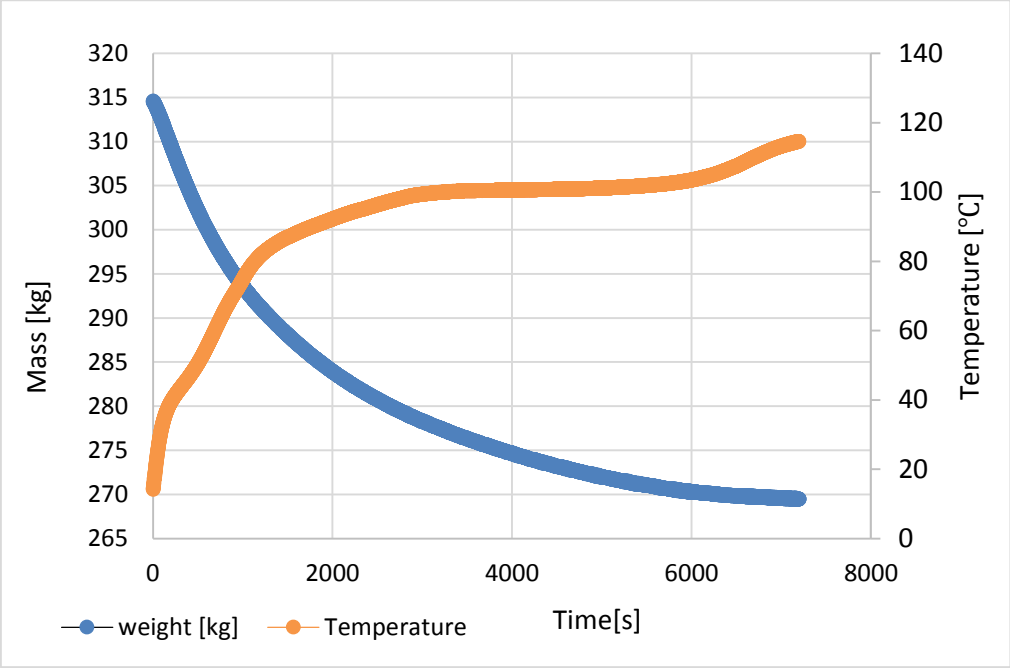

Figure 7. change in the centre temperature and mass of the sample versus time during forced convection cooking at 120℃ and 3 m/s air velocity.

We can observe in figure 7 the temperature is increasing and the mass is decreasing with time, the increasing temperature profile is because of heat transfer from the air to the sample and the decreasing mass profile is due to the mass transfer from the sample to the air. Note that the temperature increases up to the boiling point of water (100℃) where it then remains almost constant for an extended period(similar to constant-rate period in drying kinetics). This is expected due to the evaporation cooling effect. After some time, the temperature again rises as most of the water is evaporated and the energy is utilized to heat the sample (falling-rate drying period). The mass curve of the sample decreases continuously until certain time (t = 5500 s, approximately from the plot) and then flatten. At this point, there is very negligible or no mass transfer to the air.

It can be interpreted from the plot that, the flattening of the mass curve after a long processing time (t>5500 s, approximately from the plot) is because of very less or no moisture content present in the sample. At this point most of the water from the sample would have been evaporated(falling-rate drying period) and the sample is almost dry.

Figure 8 represents the plot of centre temperature of food sample versus time recorded during experimental run for three different oven temperatures.

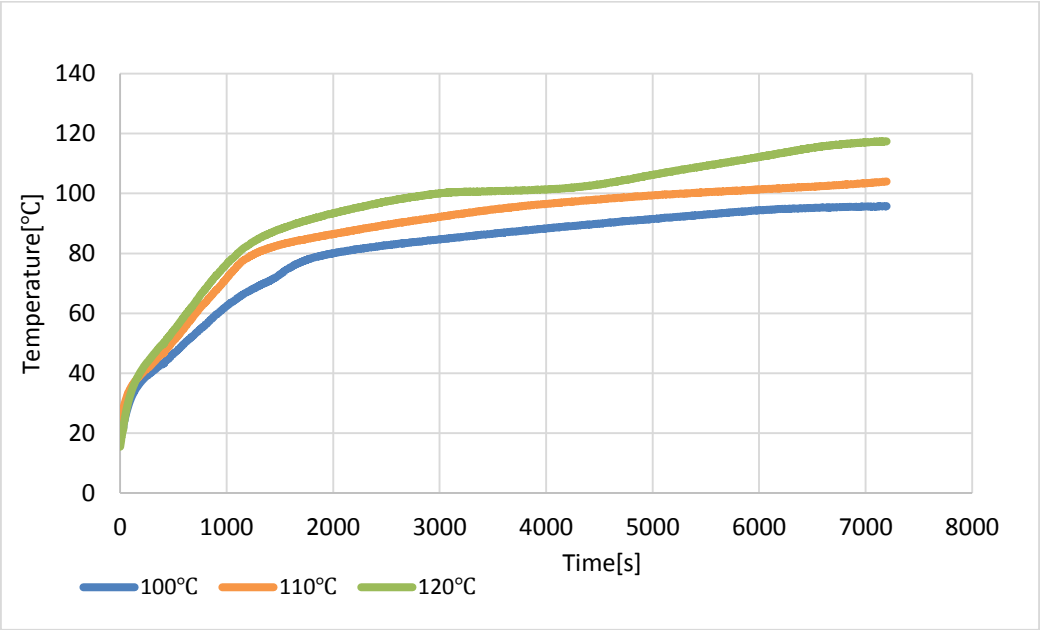

Figure 8. Temperature profile of the sample at three different oven temperature

As we can see from the figure 8, the temperature of the sample increases faster when the oven temperature is higher. The higher the set temperature of the oven the greater is the temperature gradient which is driving force for heat transfer. Meaning that heat transfer is more at higher temperatures. From the plot it is evident that the time required for the centre temperature of the sample to reach boiling point of water is less when the oven temperature is set to 120℃ than the time required when the oven temperature is set to 110℃ and 100℃. Note that the centre temperature of the sample never reaches 100℃ in the entire experimental time when the oven temperature is set to 100℃.

The fluctuations in the oven temperature over the entire experimental time is shown in figure 9. The oscillations in the oven temperature is the reason behind not having a smooth centre temperature curve of the sample. The fluctuation in the oven temperature around is ± 0.5℃.

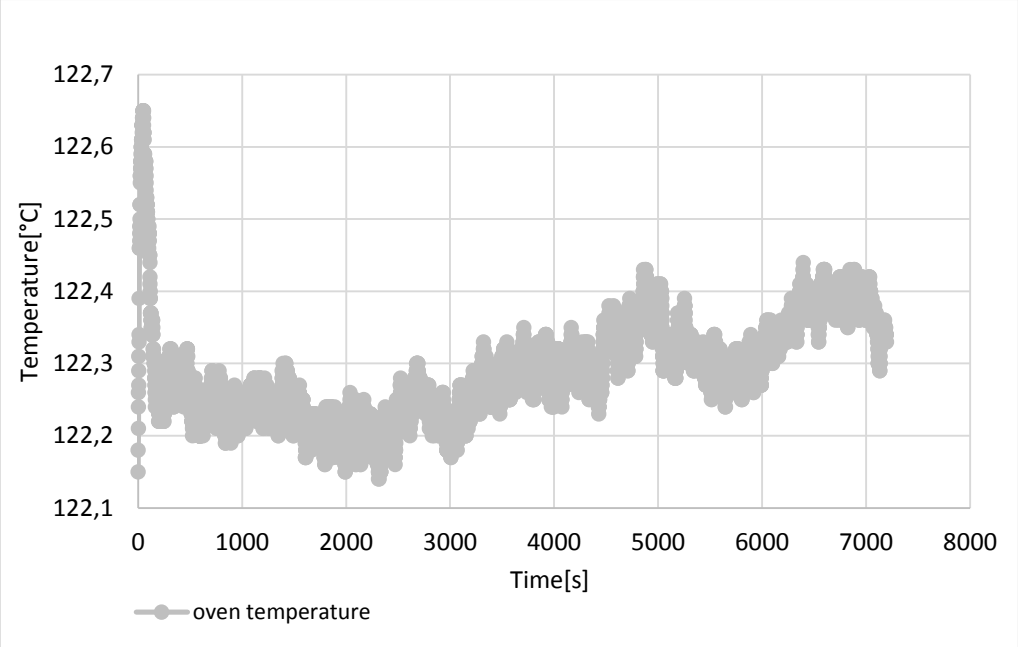

Figure 9. Fluctuations in the oven temperature over the entire experimental time

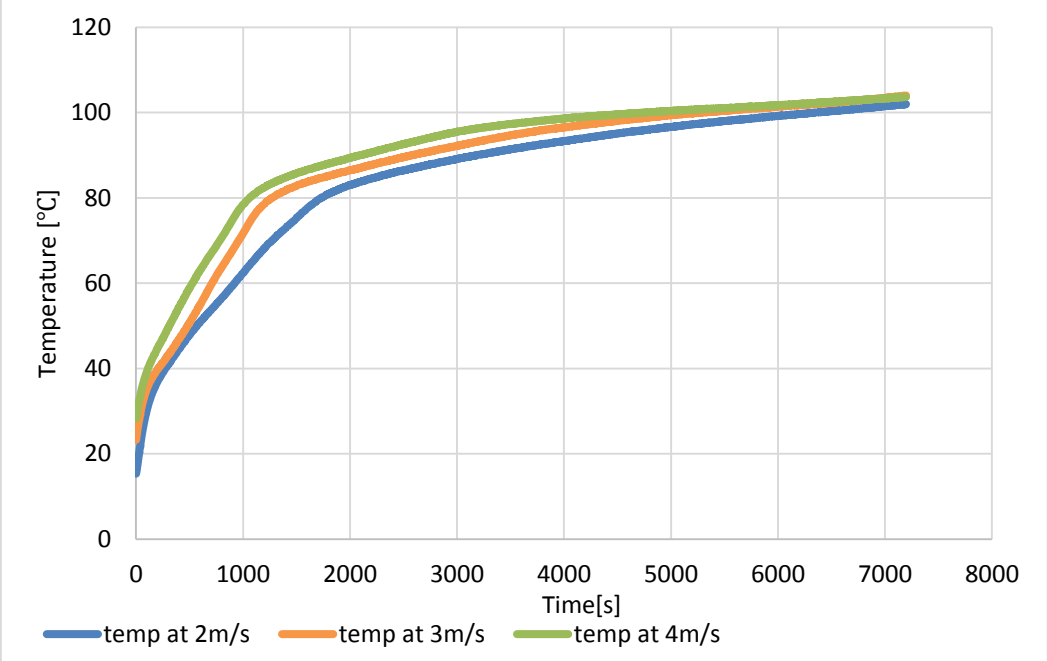

Figure 10. Temperature profile of the sample at three different air velocity

From figure 10. It is evident that at air velocity 4 m/s the heat transfer from the air stream to the sample is faster. In other words, the time required for the centre temperature of the sample to rises to 100℃ at air velocity of 4 m/s is less(t = 4000s, approximately) when compared to the time required by the sample which is heated by air at 2 m/s velocity (t= 6000sec, approximately). According to the principle, heat transfer from the fluid(air) to the solid surface is through a thin film formed at the air-solid interface. Increase in the air velocity reduces the film thickness and thereby increase heat transfer to the solid as seen in figure 10.

Figure 11. represents the mass transfer from the sample at different oven temperature and air velocity of 3 m/s. The mass[kg] at time t[s] is obtained from the experimental raw data by dividing mass at time(t) with the initial mass. The experimental results indicate that the moisture content in the food sample decreases with time.

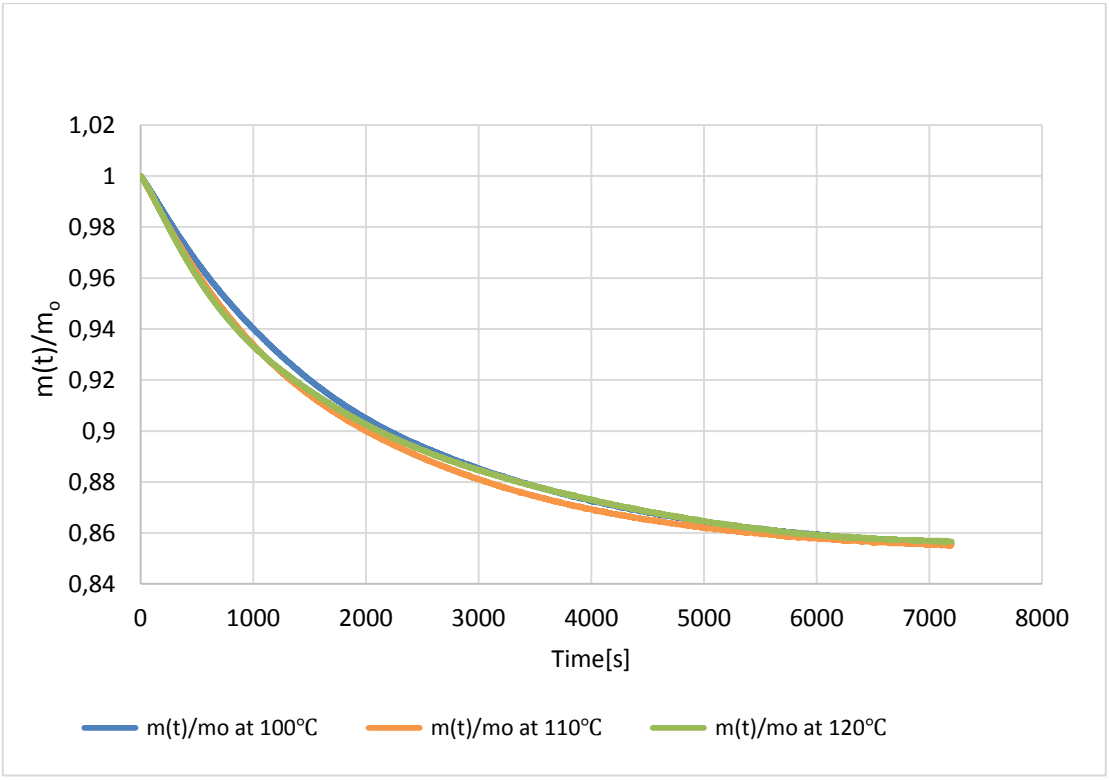

Figure 11. The moisture content profile of the samples at three different oven temperatures

In the early stages of the experimental trail (t < 300 s approximately) when the sample is placed in the oven, the surface is wet and all the heat transferred from the air to the surface is used for evaporation of water from the surface. Water from internal parts of the sample is transferred rapidly to the surface and is evaporated at a constant rate. Gradually, heat energy for evaporation is transported into the interior of the sample and moisture content continues to decrease(falling rate period). As we can see in the figure 11 mass loss curve decreases continuously over time and then flatten(when moisture content is nil). The slope of the curve describes the rate of evaporation. When comparing the mass loss curves at different oven temperatures, we can observe from figure 11 that the difference is very small, and this might be probably due to experimental uncertainty.

Figure 12. represents the mass transfer from the sample at different flow velocity and constant oven temperature of 110°C.

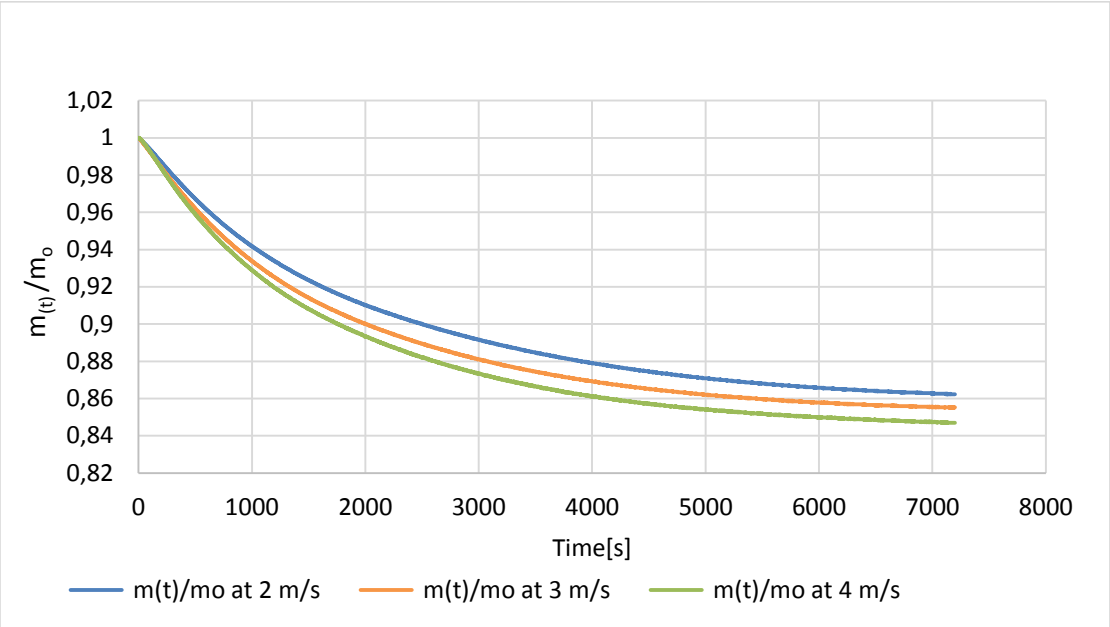

Figure 12. The moisture content profile of the sample at different flow velocity .

The transfer of moisture from the sample to the air is caused by the difference in concentration. The associated mass transport by diffusion is treated in the same way as heat transported by conduction. From figure 12, we observe that the loss of moisture increases with increasing air velocity. In principle, increase in the air velocity decreases the thickness of the boundary layer resulting in increased heat transfer to the product and thereby increasing the rate of evaporation. The loss of moisture is strongly dependent on the temperature, as the temperature increases the rate of evaporation increases (observed in figure 11). However, in figure 12. which is a plot of loss in moisture content at different air velocity and constant oven temperature we observe that the difference in the mass loss curves between different air velocity is larger than due to the difference in oven temperature(figure 11). Therefore, we can say that there might be a significant effect of air velocity on moisture transport in this system.

4.2 Determination of effective heat transfer coefficient using Yıldız method

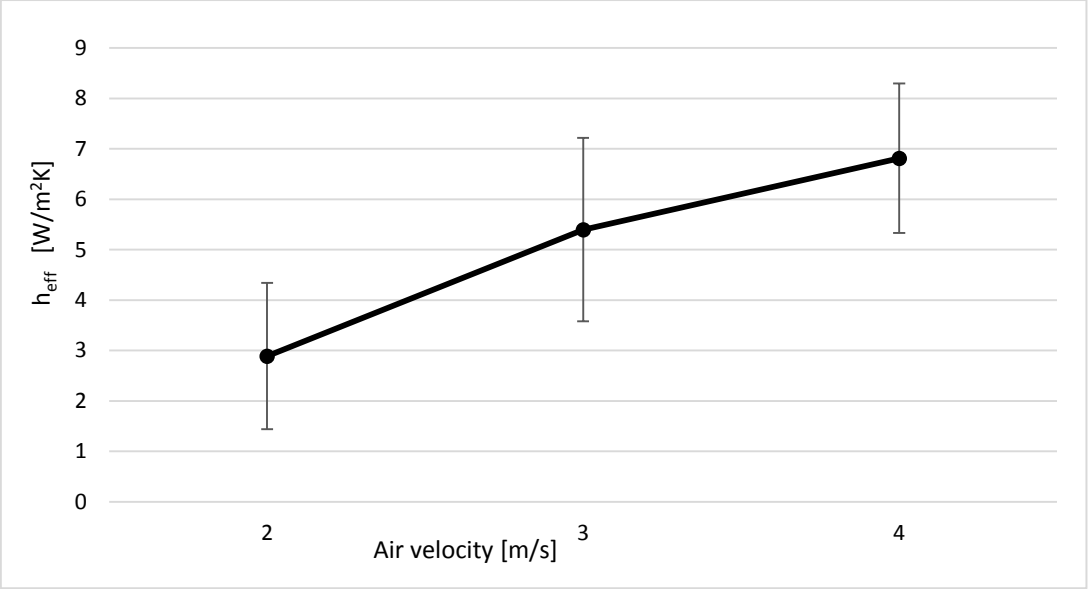

Figure 13. Effective heat transfer coefficient values estimated by Yildiz et al. (2007) method versus flow(air) velocity. The markers show the averages of the three replicates and error bars show standard deviation between the averages of the replicates.

Figure 13 shows the effective heat transfer coefficient values obtained by the Yildiz et al. (2007) method described in section 2.4.1 at different flow(air) velocity. The markers show the averages of the replicates and error bars show the standard deviation between the averages of the replicates. As we can see in figure 13 the effective heat transfer coefficient increases with increasing air velocity and we can also see that the confidence intervals are not overlapping, which means that there is statistical difference between the values. Thus, it can be concluded that the effective heat transfer coefficient varies with air velocity, which is also theoretically relevant as heat transfer coefficient has stronger dependency on air velocity. The effective heat transfer coefficient values with their standard deviations for different air velocities are presented in table 2.

Table 2: Effective heat transfer coefficient values with standard deviation and heat transfer Biot number for different air velocity.

Air velocity [m/s]	Effective heat transfer coefficient h_{eff} [W/m^{2}K]	Bi_h number
2	2.8 ± 1.4	0.02 ± 0.01
3	5.3 ± 1.8	0.04 ± 0.01
4	6.8 ± 1.4	0.06 ± 0.01

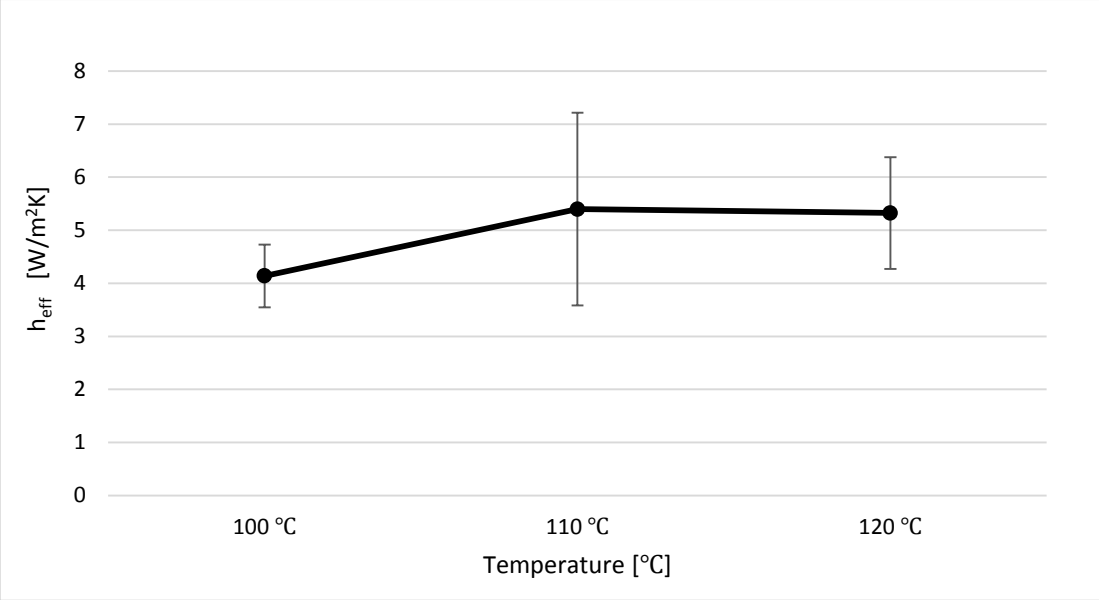

Figure 14. Effective heat transfer coefficient values estimated by Yildiz et al. (2007) method versus oven temperature. The markers show the averages of the three replicates and error bars show standard deviation between the averages of the replicates.

Figure 14 represents the effective heat transfer coefficient values obtained by the Yildiz et al. (2007) method described in section 2.4.1 at different oven temperatures. The markers show the averages of the replicates and error bars show the standard deviation between the averages of the replicates. From figure 14, it is evident that the effective heat transfer coefficient is almost same at different oven temperatures, which is reasonable as heat transfer coefficient is independent of temperature difference. According to theory, the heat transfer coefficient is dependent on thermophysical properties of the fluid and characteristics of the flow. The change in temperature causes slight change in the density and viscosity of the flow which somewhat negligible. Therefore, the effective heat transfer coefficient does not vary with temperature. Table 3. gives the effective heat transfer coefficient values with their standard deviations at different oven temperatures.

Table 3: Effective heat transfer coefficient values with standard deviation and heat transfer Biot number for different air velocity.

Air Temperature [℃]	Effective heat transfer coefficient h_{eff} [W/m²K]	Bi_h number
100	4.2 ± 1.8	0.03 ± 0.01
110	5.3 ± 1.8	0.04 ± 0.01
120	5.3± 1.0	0.04 ± 0.009

4.3 Determination of effective mass transfer coefficient using Yıldız method

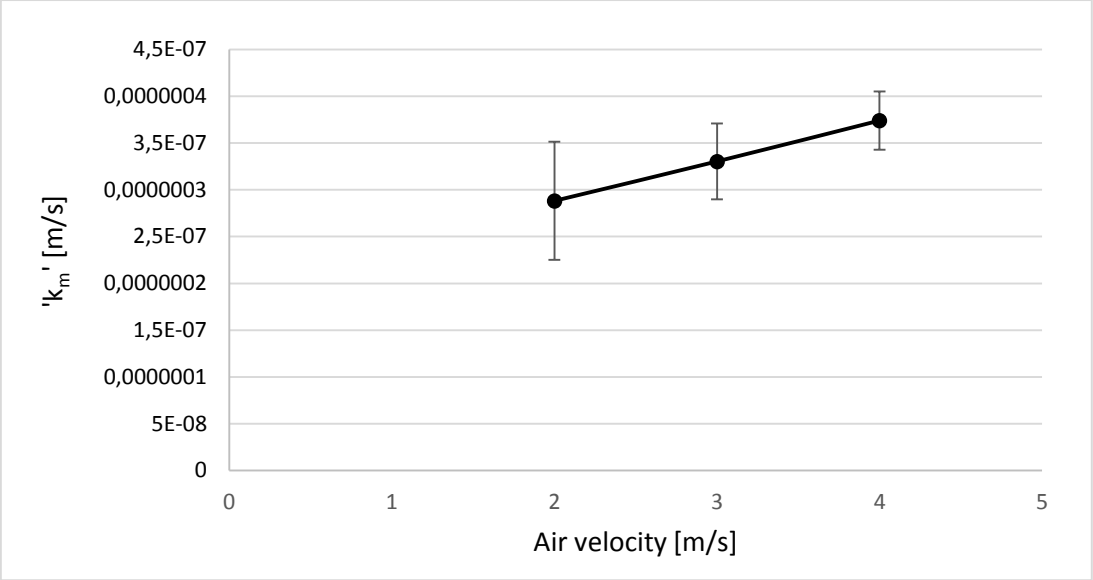

Figure 15. Effective mass transfer coefficient values estimated by Yildiz et al. (2007) method versus flow(air) velocity. The markers show the averages of the three replicates and error bars show standard deviation between the averages of the replicates.

Figure 15 is a plot of effective mass transfer coefficient obtained by the Yildiz et al. (2007) method described in section 2.4.2 against different flow(air) velocity. The markers show the averages of the replicates and error bars show the standard deviation between the averages of the replicates. In figure 15 we can see that the effective mass transfer coefficient has an increasing trend with increasing air velocity. However, when we look at the confidence intervals of 2m/s and 3m/s they are overlapping, meaning that the range of possibility in which true value for 2m/s and 3m/s lies are overlapping. Since the error bars are overlapping, we cannot conclude on a significant effect of air velocity. Effective mass transfer coefficient values with their standard deviation for different air velocities are presented in table 4. Therefore, there is only a stronger indication of difference between effective mass transfer coefficient at different air velocity, but statistically we see that there is no difference between the values.

From this, we can say that there could be difference between the values at different air velocity that we are not able to see since we have too few replicates or the method has high uncertainty associated with it, or it could be that there is actually no effect of air velocity on mass transfer.

Table 4: Effective mass transfer coefficient values with standard deviation and mass transfer Biot number for different air velocities.

Air velocity [m/s]	Effective mass transfer coefficient k_m*10^{-7}[m/s]	Bi_m number
2	2.8 ± 0.6	0.1 ± 0.01
3	3.3 ± 0.4	0.1 ± 0.02
4	3.73 ± 0.3	0.1 ± 0.01

The influence of different oven temperatures on the effective mass transfer coefficient can be better understood by plotting effective mass transfer coefficient value against temperature as represented in figure 16.

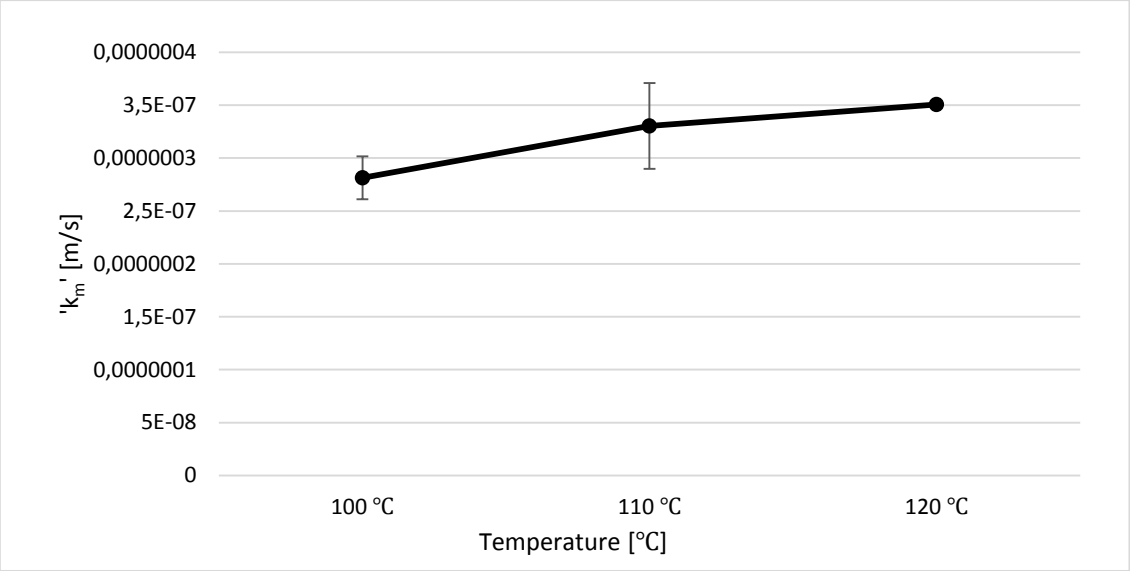

Figure 16. Effective mass transfer coefficient values estimated by Yildiz et al. (2007) method versus oven temperature. The markers show the averages of the three replicates and error bars show standard deviation between the averages of the replicates.

Figure 16 represents the effective mass transfer coefficient estimated using the Yildiz et al. (2007) method in section 2.4.2 at different oven temperatures. The markers show the averages of the replicates and error bars show the standard deviation between the averages of the replicates. We can observe in figure 16, the mass transfer coefficient seems to increase with increasing temperature but the confidence intervals of the mass transfer coefficient value at 100℃ and 110℃ are overlap indicating that there is no difference between the mass transfer coefficient obtained at 100℃ and 110℃. Note that the standard deviation of k_m value at 120℃ is not zero but it is not estimated as there was only one replicate. It was not possible to repeat the experimental trail for 120℃ oven temperature because of some technical issue and COVID-19 crisis. The effective mass coefficient for different oven temperatures along with their standard deviation are given in Table 5. There is only indication of difference between the effective mass transfer coefficient values at different temperatures but statistically there is no significant difference. From this we can say that there is no statistically significant effect. Note that this is not the same as saying that there is no such effect. The results might be either due to 'k_m' not varying with temperature or that the variation is smaller than what we can distinguish with our method.

Table 5: Effective mass transfer coefficient values with standard deviation and mass transfer Biot number for different oven temperatures.

Air Temperature [℃]	Effective mass transfer coefficient k_m*10^{-7}[m/s]	Bi_m number
100	2.8 ± 0.2	0.1± 0.01

110	3.3 ± 0.4	0.1 ± 0.02
120	3.5	0.175

4.4 Comparison of the experimentally determined h and Km values with the empirically predicted values using correlations

The empirical calculations of the heat transfer coefficient and mass transfer coefficient using Nusselt correlation discussed in section 2.4.3 and 2.4.5 respectively, can be found in appendix D-E. The coefficient values calculated from the Nusselt correlations are compared with the values from the experimental method in subsections below.

4.4.1 Heat transfer coefficient

Table 6. and table 7. shows a comparison between experimentally estimated 'h_{eff}' value and Nusselt correlation 'h' value for different geometry using the correlations in section 2.4.3 at different oven temperatures and flow(air) velocity, respectively.

Table 6. Comparing the experimental h_{eff} and empirical 'h' values at different oven temperature.

Air Temperature[℃]	Empirical h [W/m²K] (*flow around a sphere)*	Empirical h [W/m²K] (*flow around a cylinder)*	Empirical h [W/m²K] *(flow over cylinder of noncircular cross section)*	Experimental h_{eff} [W/m²K]
100	40.2	77.8	76.9	4.2 ± 1.85
110	40.2	77.8	75.8	5.3 ± 1.81
120	40.4	77.1	75.9	5.3 ± 1.05

Table 7. Comparing the experimental h_{eff} and empirical 'h' values at different air velocity.

Air velocity [m/s]	Empirical h [W/m²K] (*flow around a sphere)*	Empirical h [W/m²K] (*flow around a cylinder)*	Empirical h [W/m²K] *(flow over cylinder of noncircular cross section)*	Experimental h_{eff} [W/m²K]
2	34.9	61.8	62.7	2.8 ± 1.44
3	40.2	77.8	75.8	5.3 ± 1.81
4	44.7	90.6	86.6	6.8 ± 1.48

4.4.2 Mass transfer coefficient

The table 8. and table 9. represents a comparison between experimentally estimated 'k_m' value and Nusselt correlation 'k_m' value for different geometry using correlations described in section 2.4.4 at different oven temperatures and flow(air) velocity.

Table 8. Comparing the experimental and empirical 'k_m' values at different oven temperature.

Air Temperature[℃]	**Empirical k_m *10^{-2} [m/s] (*flow around a sphere)***	**Empirical k_m *10^{-2} [m/s] (*flow around a cylinder)***	**Empirical k_m *10^{-2} [m/s](*flow over cylinder of noncircular cross section)***	**Experimental k_m *10^{-7} [m/s]**
100	4.2	8.3	8.1	2.8 ± 0.20
110	4.3	8.3	8.1	3.3 ± 0.40
120	4.4	8.4	8.2	3.5

Table 9. Comparing the experimental and empirical 'k_m' values at different air velocity.

Air velocity [m/s]	**Empirical k_m *10^{-2} [m/s] (*flow around a sphere)***	**Empirical k_m *10^{-2} [m/s] (*flow around a cylinder)***	**Empirical k_m *10^{-2} [m/s](*flow over cylinder of noncircular cross section)***	**Experimental k_m *10^{-7} [m/s]**
2	3.7	6.6	6.7	2.88± 0.63
3	4.3	8.3	8.1	3.3 ± 0.40
4	4.8	9.7	9.3	3.7 ± 0.31

We can observe from the above comparisons (table 6-9) that the experimentally estimated 'h_{eff}' and 'k_m' values are very low when compared with the values obtained using Nusselt correlations. This means that there is a huge difference between the coefficient values determined using the experimental approach and the correlations. The Nusselt correlations gives the convective heat transfer and mass transfer coefficient values but whereas the experimental method determines the effective convective heat and mass transfer coefficient values. In the experimental approach the heat transfer rate is greatly influenced by the effect of evaporation cooling and hence the effective heat transfer and mass transfer coefficient values are lower than the true values. The magnitude of convective heat transfer coefficient 'h' during forced air convection is between 10 – 100 (W/m^2 K) (Singh and Heldman, 2014).

As the experimentally estimated value of heat transfer and mass transfer coefficients are very low, it is not possible to conclude on which of the three Nusselt correlations (Eq 21, Eq 22 or Eq 23) is appropriate with regard to the geometry of the sample in this study for empirically calculating heat and mass transfer coefficients. However, when comparing the experimental values and Nusselt correlation values we can observe that they have a similar trend. Note that the value obtained using Nusselt correlations for flow over cylinder of noncircular cross section and flow around a cylinder are almost same.

5. Limitations

1. Limitations in the experimental setup: The temperature of the oven which is stabilized before starting the experiment varies when the door of the oven is opened to place the sample inside, the air flow around each slice of potato is not identical as shown in figure 5, the weighing balance measuring the mass loss over the entire experimental time is not infinitely sensitive, it was tricky to position the thermocouple exactly at the geometric centre of the potato slice to precisely measure the centre temperature, the number of replicates were limited due to time constraints.
2. Limitations in the Yıldız et al. (2007) method: The method is most likely applicable to limited geometry of the food sample, deals with only the sensible heat and ignores the latent heat of evaporation during the estimation of coefficients, the method is extremely sensitive to small deviations in the experimental data, measures the effective heat and mass transfer coefficient, most importantly Yıldız et al. (2007) method assumes that the thermal conductivity 'k' (W/mK) and thermal diffusivity 'α' (m^2/s) are independent of temperature, the method does not take into account the position of the thermocouple measuring the centre temperature of the product.
3. With the limited number of replicates, it was difficult to find significant statistical differences between the values and conclude. When determining the effective mass transfer coefficient, the Yıldız et al. (2007) method was very sensitive to the experimental data and hence required some modifications to obtain the mass transfer coefficient value.

6. Conclusion

- The investigation of effective heat transfer and mass transfer coefficients during forced air convection at different oven temperatures and flow(air) velocity using Yıldız et al. (2007) approach resulted in low coefficient values.
- The effective heat transfer and mass transfer coefficient remains almost same with increasing oven temperature. However, with increasing air velocity the effective heat transfer coefficient increased significantly but there is no statistically significant influence on the effective mass transfer coefficient
- Comparing the measurements from the Yıldız et al. (2007) method and the empirical correlations, we observe a good agreement between the measurements with respect to the trend they follow when increasing the oven temperature and air velocity. However, there is large difference between the experimentally and empirically obtained values. This is expected since the method of Yıldız et al. (2007) method determines the effective heat and mass transfer coefficient values which is lower than the convective heat and mass transfer coefficient.

7. Future Research

The study conducted was time bound and hence included some limitations. Therefore, some suggestions for future research would be,

- Performing investigation with a greater number of replicates to reduce experimental uncertainty.
- Investigate the impact on mass transfer parameter by increasing the difference between the set flow(air) velocity, for example at 2m/s, 4m/s and 6m/s.
- Change the dimension of the food sample and investigate on the heat and mass transfer effects.
- Estimating the heat transfer and mass transfer parameters using a different method and then compare the results to better understand the effectiveness and accuracy of the method.

References

Singh, R. and Heldman, D. (2014). *Introduction to food engineering*. 5th ed. Academic Press.

Toledo, Romeo T. (2007). *Fundamentals of food process engineering*. 3rd ed. Springer.

Heldman R. and Lund B. (2007). *Handbook of food engineering*. 2nd ed. CRC Press.

Yıldız, A., Koray Palazoğlu, T. and Erdoğdu, F. (2007). Determination of heat and mass transfer parameters during frying of potato slices. *Journal of Food Engineering*, 79(1), pp.11-17.

Bergman, T., Lavine, A., Incropera, F., and Dewitt, D. (2018). *Incropera's Principles of Heat and Mass Transfer*. John Wiley & Sons Inc.

Bird, R.B., Stewart, W.E. & Lightfoot, E.N. (2002). *Transport phenomena*. 2nded. New York: Wiley.

Brodkey, R.S. and Hershey H.C. (1988). *Transport Phenomena: A Unified Approach.* McGraw-Hill.

Enayatollahi, R., Nates, R. and Anderson, T. (2017). The analogy between heat and mass transfer in low temperature crossflow evaporation. *International Communications in Heat and Mass Transfer*, 86(1), pp.126-130.

Skjoldebrand, C. (1980). Convection oven frying heat and mass transport in the product. *Journal of Food Science*, 45(5), pp.1347-1353.

Feyissa, A.H, 2011, '*Robust modelling of heat and mass transfer in processing of solid foods*', PhD thesis, Technical University of Denmark, Denmark.

Carson, J.K. , Willix, J. and North, M.F. (2006). Measurements of heat transfer coefficients within convection ovens. *Journal of Food Engineering*, 72(3), pp. 293–301.

Sablani, S.S. (2009). 'Measurement of surface heat transfer coefficient', in Rahman, M.S. (ed.) *Food properties handbook*. CRC Press: Florida, pp. 83-95.

Safari, A., Salamat, R. and Baik, O. (2018). A review on heat and mass transfer coefficients during deep-fat frying: Determination methods and influencing factors. *Journal of Food Engineering,* 230, pp.114-123.

Kondjoyan, A. and Daudin, J.D. (1997). Heat and mass transfer coefficients at the surface of a pork hindquarter. *Journal of Food Engineering*, 32, pp. 225–240.

Zheng, L., Delgado, A. and Sun, D. (2009). 'Surface heat transfer coefficients with and without phase change', in Rahman, M.S. (ed.) *Food properties handbook*. CRC Press: Florida, pp. 717-758.

Appendices

Appendix A: Thermophysical properties of potato.(Yıldız et al. (2007)

Physical property	Value
Thermal conductivity, k (W/mK)	0.554
Density, ρ (kg/m^3)	1090
Specific heat, Cp (J/kgK)	3517

Appendix B: Constants for the circular cylinder in cross flow.(Bergman and Lavine, 2018)

ReD	C	m
0.4 - 4	0.989	0.330
4 - 40	0.911	0.385
40 - 4000	0.683	0.466
4000 - 40000	0.193	0.618
40000 - 400000	0.027	0.805

Appendix C: Determination of diffusivity coefficient for theoretical estimation of mass transfer coefficient at different oven temperatures. (Brodkey and Hershey, 1988)

The diffusivity coefficient of water vapor in air at 1atm pressure and different average bulk fluid(air) temperatures is estimated using the equation,

$$D = D_o \frac{P_0}{P} \left(\frac{T}{T_0}\right)^n$$

Where diffusivity coefficient (D_o) is known at standard temperature (T_o) and standard pressure, (P_o) and the exponent n is 1.75 if the pressure less than approximately 5 atm. Diffusivity coefficient at 1atm pressure and 0°C temperature is $0.219*10^{-4}$ m^2/s.

At 60°C and 1atm pressure,

$$D = D_o \frac{P_0}{P} \left(\frac{T}{T_0}\right)^n = 0.219 \cdot 10^{-4}\ (m^2/s) \cdot \frac{1atm}{1atm} \left(\frac{333.15\ K}{273.15\ K}\right)^{1.75} = 0.314 \cdot 10^{-4}\ m^2/s$$

At 65°C and 1atm pressure,

$$D = D_o \frac{P_0}{P} \left(\frac{T}{T_0}\right)^n = 0.219 \cdot 10^{-4}\ (m^2/s) \cdot \frac{1atm}{1atm} \left(\frac{338.15\ K}{273.15\ K}\right)^{1.75} = 0.319 \cdot 10^{-4}\ m^2/s$$

At 70°C and 1atm pressure,

$$D = D_o \frac{P_0}{P} \left(\frac{T}{T_0}\right)^n = 0.219 \cdot 10^{-4}\ (m^2/s) \cdot \frac{1atm}{1atm} \left(\frac{343.15\ K}{273.15\ K}\right)^{1.75} = 0.327 \cdot 10^{-4}\ m^2/s$$

Appendix D: Calculations of the heat transfer coefficient using empirical correlations

The Nusselt correlation for estimating the heat transfer coefficient is chosen depending on the type of fluid flow and geometry of the object.

Dimension of the solid = 10mm·10mm·60mm
dc = $(10 \cdot 10^{-3}/2)$ = 0.005m
Velocity of air = 3m/s
Temperature of air = 100℃
Temperature of the sample 'T_s' = 20℃

All physical properties must be evaluated at average bulk fluid temperature, T_f.
$T_f = [(T_s+T_{air})/2] = (20+100)/2 = 60℃$

The values of thermophysical properties of air are taken from appendix A.4.4, Singh and Heldmen, 2014.
Viscosity 'μ' = $19.907 \cdot 10^{-6}$ (Ns/m^2)
Specific heat 'Cp' = 1017 (J/[KgK])
Thermal conductivity 'k' = 0.0279 (W/[mK])
Density ' ρ' = 1.025 (kg/m^3)

First determine the Reynolds number and Prandtl's number,

$N_{Re} = \rho u d_c/\mu = [0.916\ (kg/m^3) \cdot 3(m/s) \cdot 0.005(m)] / [21.673 \cdot 10^{-6}\ (Ns/m^2)] = 772$

$N_{Pr} = \mu C_p/k = [21.673 \cdot 10^{-6}\ (Ns/m^2) \cdot 1022\ (J/kgK)] / [0.0307\ (W/mK)] = 0.72$

The Nusselt correlation for flow around a sphere is given by,

$$N_{Nu} = 2.0 + 0.6(N_{Re})^{0.5}(N_{Pr})^{0.33}$$

By substituting N_{Re} and N_{Pr} values,

$N_{Nu} = 2.0 + 0.6(N_{Re})^{0.5}(N_{Pr})^{0.33} = 2.0 + 0.6 \cdot (772)^{0.5} \cdot (0.72)^{0.33} = 7.206$

$N_{Nu} = \frac{h\, d_c}{k}$, h = [7.206 · 0.0279 (W/mK)] / 0.005m = 40.2 W/m^2K

Nusselt number correlation for flow around a cylinder is,

$$N_{Nu} = (0.4N_{Re}^{1/2} + 0.06N_{Re}^{2/3})(N_{Pr})^{0.4}\left(\frac{\mu_b}{\mu_w}\right)^{\frac{1}{4}}$$

All physical properties except u_w, must be evaluated at average bulk fluid temperature,

Viscosity at wall temperature 'μ_w' = $21.452 \cdot 10^{-6}(Ns/m^2)$

$N_{Re} = \rho u d_c/\mu = [0.916\ (kg/m^3) \cdot 3(m/s) \cdot 0.005(m)] / [21.673 \cdot 10^{-6}\ (Ns/m^2)] = 772$

$N_{Pr} = \mu C_p/k = [21.673 \cdot 10^{-6}\ (Ns/m^2) \cdot 1022\ (J/kgK)] / [0.0307\ (W/mK)] = 0.72$

By substituting N_{Re} and N_{Pr} values,

$N_{Nu} = (0.4N_{Re}^{1/2}+0.06N_{Re}^{2/3})(N_{Pr})^{0.4}\left(\frac{\mu_b}{\mu_w}\right)^{1/4}$

$N_{Nu} = (0.4\cdot (772)^{1/2}+0.06\cdot (772)^{2/3}\cdot (0.72)^{0.4}\cdot \left(\frac{19.907\cdot 10-6}{21.452\cdot 10-6}\right)^{1/4} = 13.9$

$N_{Nu} = \frac{h\, d_c}{k}$ = h = [13.957 · 0.0279 (W/mK)] / 0.005m = 75.9 W/m^{2}K

Nusselt correlation for flow over cylinder of noncircular cross section is,

$$N_{Nu} = C(N_{Re})^m(N_{Pr})^{1/3}$$

The value of constants C and m are found in appendix B and substituting the N_{Re} and N_{Pr} values.

$N_{Re} = \rho u d_c/\mu$ = [0.916 (kg/m^3) · 3(m/s) · 0.005(m)] / [21.673·10^{-6} (Ns/m^2)] = 772

$N_{Pr} = \mu C_p/k$ = [21.673·10^{-6} (Ns/m^2) · 1022 (J/kgK)] / [0.0307 (W/mK)] = 0.72

$N_{Nu} = C(N_{Re})^m(N_{Pr})^{1/3} = 0.683\cdot (772)^{0.466}\cdot (0.72)^{1/3} = 13.6$

$N_{Nu} = \frac{h\, d_c}{k}$ = h = [13.605 · 0.0279 (W/mK)] / 0.005m = 77.8 W/m^{2}K

Appendix E: Calculations of the mass transfer coefficient using correlations analogous to the heat transfer correlations

The Sherwood number correlation for flow around a sphere is given by,

$$N_{Sh} = 2.0+0.6(N_{Re})^{0.5}(N_{Sc})^{0.33}$$

Dimension of the solid = 10mm*10mm*60mm

dc = $(10\cdot10^{-3}/2)$ = 0.005m

Velocity of air = 3m/s

Temperature of air = 100℃

Temperature of the sample 'T_s' = 20℃

All physical properties must be evaluated at average bulk fluid temperature, T_f.

T_f =[$(T_s+T_{air})/2$] = (20+100)/2 = 60℃

The values of thermophysical properties of air are taken from appendix A.4.4, Singh and Heldmen, 2014.

Viscosity 'μ' = $19.907\cdot10^{-6}$ (Ns/m^2)

Density ' ρ' = 1.025 (kg/m^3)

Diffusivity of water vapor in air 'D_{AB}' = $0.314\cdot10^{-4}$ (m^2/s)

First determine the Reynolds number and Schmidt's number,

$N_{Re} = \rho u d_c/\mu$ = [1.025 (kg/m^3) · 3(m/s) · 0.005(m)] / [$19.907\cdot10^{-6}$ (Ns/m^2)] = 772

$N_{Sc} = \mu/\rho D_{AB}$ = [$19.907\cdot10^{-6}$ (Ns/m^2)] / [1.025 (kg/m^3) · $0.314\cdot10^{-4}$ (m^2/s)] = 0.61

$N_{Sh} = 2.0+0.6(N_{Re})^{0.5}(N_{Sc})^{0.33} = 2.0 + 0.6\cdot (772)^{0.5} \cdot (0.61)^{0.33}$ = 6.8

$N_{Sh} = \frac{k_m \cdot d_C}{D_{AB}}$, k_m = [$0.314\cdot10^{-4}$ (m^2/s) · 6.836] / 0.005m = $4.2\cdot10^{-2}$ m/s

The Sherwood number correlation for flow around a cylinder is given by,

$$N_{Sh} = (0.4N_{Re}^{1/2}+0.06N_{Re}^{2/3})(N_{Sc})^{0.4}\left(\frac{\mu_b}{\mu_w}\right)^{1/4} \cdot N_{Pr}^{-1/3} \cdot N_{Sc}^{1/3}$$

All physical properties except u_w, must be evaluated at average bulk fluid temperature,

Viscosity at wall temperature 'μ_w' = $21.452\cdot10^{-6}$(Ns/m^2)

By substituting N_{Re} and N_{Sc} values,

$N_{Re} = \rho u d_c/\mu$ = [1.025 (kg/m^3) · 3(m/s) · 0.005(m)] / [$19.907\cdot10^{-6}$ (Ns/m^2)] = 772

$N_{Sc} = \mu/\rho D_{AB}$ = [$19.907\cdot10^{-6}$ (Ns/m^2)] / [1.025 (kg/m^3) · $0.314\cdot10^{-4}$ (m^2/s)] = 0.61

$N_{Sh} = (0.4N_{Re}^{1/2}+0.06N_{Re}^{2/3})(N_{Sc})^{0.4}\left(\frac{\mu_b}{\mu_w}\right)^{1/4} \cdot N_{Pr}^{-1/3} \cdot N_{Sc}^{1/3}$

$N_{Sh} = (0.4) \cdot (772)^{1/2}+0.06\cdot (772)^{2/3}\cdot (0.61)^{0.4}\left(\frac{19.907\cdot10-6}{21.452\cdot10-6}\right)^{1/4} \cdot (0.72)^{-1/3} \cdot (0.61)^{1/3}$ = 13.2

$N_{Sh} = \frac{k_m \cdot d_C}{D_{AB}}$, k_m = [0.314·10^{-4} (m^2/s) ·13.240] / 0.005m = 8.1·10^{-2} m/s

Nusselt correlation for flow over cylinder of noncircular cross section is,

$$N_{Sh} = C(N_{Re})^m(N_{Sc})^{1/3}$$

The value of constants C and m are found in appendix B and substituting the N_{Re} and N_{Sc} values.

$N_{Re} = \rho u d_c/\mu$ = [1.025 (kg/m^3) · 3(m/s) · 0.005(m)] / [19.907·10^{-6} (Ns/m^2)] = 772

$N_{Sc} = \mu/\rho D_{AB}$ = [19.907·10^{-6} (Ns/m^2)] / [1.025 (kg/m^3) · 0.314·10^{-4} (m^2/s)] = 0.61

$N_{Sh} = C(N_{Re})^m(N_{Sc})^{1/3}$ = 0.683· (772) $^{0.466}$ · $(0.61)^{1/3}$ = 12.9

$N_{Sh} = \frac{k_m \cdot d_C}{D_{AB}}$, k_m = [0.314·10^{-4} (m^2/s) ·12.900] / 0.005m = 8.3·10^{-2} m/s

Appendix F: Additional pictures of experimental setup

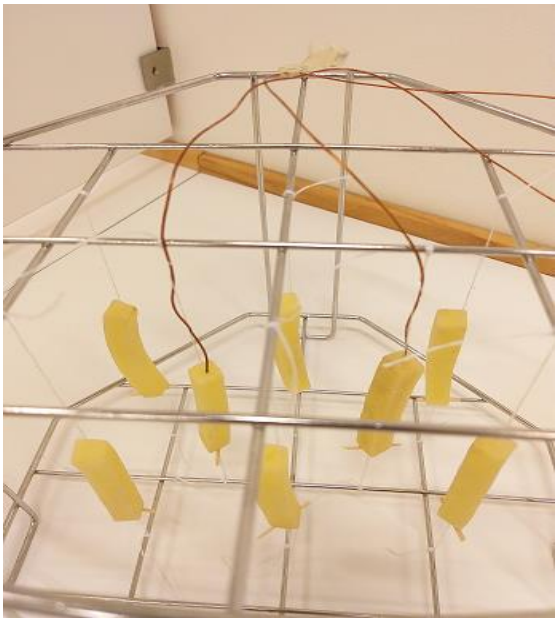

(a)

(b)

Figure (a) and (b): The thermocouples sewn into the potato slice to record the centre temperature changes and fastened at the bottom with the help of toothpick. The potato slices are then tied to the stainless-steel grill rack in a suspended manner.